Polymer Chemistry

Accepted Manuscript

ROYAL SOCIETY OF CHEMISTRY

www.rsc.org/polymers

Journal Name

RSCPublishing

Article

Modulation and Evaluation of Charge Carrier Mobility in Polymer Alloy of Polythiophene and Insulating Matrix with Electron Accepting Molecule

Cite this: DOI: 10.1039/x0xx00000x

Received 00th January 2012,
Accepted 00th January 2012

DOI: 10.1039/x0xx00000x

www.rsc.org/

Takahiro Fukumatsu,[a] Akinori Saeki,*[a] and Shu Seki*[a,b]

Modulation of backbone conformation and aggregation behaviour of conjugated polymer is of great importance to aid the design of efficient organic semiconductors. We report the optical and electronic properties of polymer alloys comprising regioregular poly(3-hexylthiophene) (P3HT) and insulating matrix of polystyrene (PS) or poly(methyl methacrylate) (PMMA). Charge carrier mobilities in the polymer alloys were evaluated by flash-photolysis time-resolved microwave conductivity (FP-TRMC) and transient absorption spectroscopy (TAS) and found to vary with the matrix and blend ratio. Photoabsorption and fluorescence spectroscopies provide a rationale for the conformation and aggregation of P3HT. Phase separations in the blend films were investigated by atomic force microscopy to support the FP-TRMC results. Moreover, we design styrene-perylenediimide (PDI) copolymer (St-PDI) and methyl methacrylate-PDI copolymer (MMA-PDI), which simultaneously allow the dispersion of electron-accepting PDI removing the contribution of electron mobility, spectroscopic probe of PDI radical anion, and modulation of electronic feature of P3HT. The hole mobility of 0.07 $cm^2V^{-1}s^{-1}$ was determined in the P3HT:St-PDI by FP-TRMC and TAS. The proposed polymer alloy approach is useful and applicable to a wide range of p-type polymers to investigate their matrix-induced change of charge transport property.

Introduction

Conjugated polymers have started to be deployed in the field of flexible electronics such as organic photovoltaic cells (OPV),[1-7] organic field effect transistor (OFET),[8-14] and organic light emitting diode (OLED).[15-20] Regioregular poly(3-hexylthiophene), P3HT is one of the most promising p-type polymers in OPV[21-24] and OFET.[25-28] High hole mobility in P3HT originates from the two-dimensional lamellar crystallites concomitant with its planar backbone.[29-31] Therefore controlling the conformation and high-order self-assembly of P3HT leverages the improvement of the electronic property.

A polymer alloy comprising multiple polymers is a premier engineering plastic with excellent hardness and long-term durability. In organic electronics, all-polymer solar cell composed of p-type and n-type polymers, a counterpart of the wide-spread polymer: fullerene OPV, has experienced marked growth in the number of researches.[32-34] In addition, since Jenekhe *et. al.*have reported the FET charge carrier mobility of P3HT/polystyrene,[35] polymer alloys of P3HT and insulating polymer have garnered intense attention in OFET, because their stability and tolerance of oxidation are expected to be higher than pristine P3HT. Goffri *et al.* have reported the FET mobilities in polymer alloys of P3HT and crystalline polyethylene (PE) or amorphous polystyrene (PS).[36] Most interestingly, the polymer alloy of PE blended with only 10 wt% P3HT showed the high FET mobility of 6×10^{-2} $cm^2 V^{-1}s^{-1}$ comparable to that of pristine P3HT (~ 10^{-1} $cm^2 V^{-1}s^{-1}$). Rendering vertical phase separation plays a key role to concentrate the low-content P3HT on the surface of gate insulator. Qui *et al.* revealed that the fibrous P3HT in the insulating PS matrix efficiently form percolation network, thus leading to the high FET mobility.[37] They used

[a]*Department of Applied Chemistry, Graduate School of Engineering, Osaka University, 2-1 Yamadaoka, Suita, Osaka 565-0871, Japan.* [b]*Department of Molecular Engineering, Graduate School of Engineering, Kyoto University, Nishikyo-ku, Kyoto 615-8510, Japan. E-mail: saeki@chem.eng.osaka-u.ac.jp , seki@moleng.kyoto-u.ac.jp*

† Electronic supplementary information (ESI) available: Experimental and Figs S1-S2. See DOI: 10.1039/XXXXXXXXXX.

CH_2Cl_2 as a solvent of P3HT:PS mixture, which is rather poor solvent for P3HT. Therefore, it is suggested that large portions of the P3HT molecules have solidified at room temperature, to form nanofibers, which are selectively connected during spin-coating.

In contrast, the use of good solvent would lead to more dispersed P3HT domain, impeding the long-range charge transport pathway unsuitable for FET characterization. In analogy, covering semiconducting polymer wire by aliphatic chain through chemical synthesis is another approach of isolation.[38,39] For the electrical evaluation of these semiconductors embedded in insulators, non-contact time-resolved microwave conductivity (TRMC)[40-44] has advantage over the most common direct-current methods like FET, since TRMC can probe local charge motion by alternating-current electric field of microwave.

Here, we report the polymer alloys of P3HT and PS or poly(methyl methacrylate) (PMMA) studied by photoabsorption and fluorescence spectroscopies, flash-photolysis (FP-)TRMC, and atomic force microscopy (AFM). Amorphous PS and PMMA with good transparency and film quality are unresponsive to FP-TRMC and suitable for optical spectroscopy. Besides, the large difference in surface energies of PS and PMMA (26 and 44 mJ m^{-2}, respectively) enable to tune the miscibility with P3HT (20 mJ m^{-2})[45] and influence its conformation and aggregation behaviour. Furthermore, we designed and synthesized a styrene-perylenediimide (St-PDI) and methylmethacrylate-perylenediimide (MMA-PDI) copolymers, which allows the complete non-contact evaluation of hole mobility of p-type polymer in an insulating matrix using FP-TRMC and transient absorption spectroscopy (TAS). This method make it possible to facilely evaluate the local hole mobility of various p-type polymers, giving access to an underlying electronic features associated with polymer conformation.

Experimental

Materials and general measurements. Synthesis of PDI monomer and copolymers are shown in Scheme 1. The synthetic details of PDI monomer and its precursors (**1**),[46,47] (**2**), (**3**),[48] and (**4**) are provided in Electronic Supporting Information (ESI). Reagents were purchased from Tokyo Chemical Incorporation (TCI), unless otherwise noted. PS (weight-averaged molecular weight, M_w = 280 kg mol^{-1}), PMMA (M_w = 350 kg mol^{-1}), and regioregular P3HT (M_w = 42 kg mol^{-1}, Plexcore OS 2100, regioregularity >98%) were purchased from Aldrich and used without further purification. Chlorobenzene was purchased from Kishida Kagaku Co. and used as received. Film samples were prepared by drop-casting from chlorobenzene solutions (totally ca. 10 wt%) onto a quartz substrate. They were dried for 1h in vacuum at room temperature. No thermal annealing was applied. ^{1}H NMR spectra were recorded on a 400 MHz JEOL Spectrometer. All the chemical shifts were referenced to $(CH_3)_4Si$ (TMS; δ = 0 ppm). Elemental analysis was performed for the copolymers with a Yanagimoto Mfg. Co., Ltd. YANACO CHN CORDER (MT-5) for C, H, and N elements. The molecular weights of the polymers were measured by gel permeation chromatography (GPC, Hitachi, L-2130, L-2350, L-2455) in tetrahydrofuran solution calibrated against polystyrene standards. Photoabsorption spectra were recorded on a JASCO V-570 spectrophotometer and the fluorescence spectra (λ_{ex} = 355 nm) in solution and solid state were

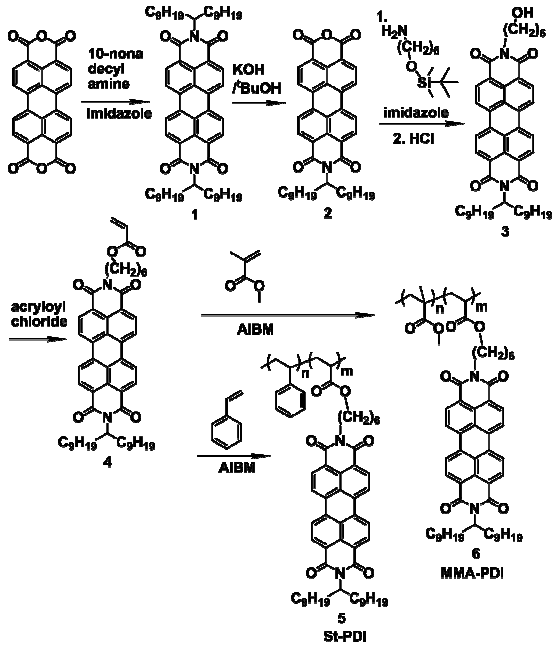

Scheme 1. Synthesis of Swallow-tail PDI (**1**), St-PDI (**5**), and MMA-PDI (**6**) copolymer.

recorded on a Hitachi F-2700. Atomic force miscopy (AFM) was performed on a Buker MultiMode 8 with ScanAsyst mode.

Time-resolved microwave conductivity (TRMC) and transient absorption spectroscopy (TAS).[42,43] The third harmonic generation (THG; 355 nm) of a Nd:YAG laser (Spectra-Physics Inc., INDI, 5-8 ns pulse duration, 10 Hz) and X-band microwave (ca. 9 GHz, 3mW) were used as an excitation source and a probe, respectively. The laser power was fixed at 4.6×10^{15} photons cm^{-2} $pulse^{-1}$. The value of conductivity is converted to the product of the quantum yield : ϕ and the sum of charge carrier mobilities : $\Sigma\mu$, by $\phi\Sigma\mu = \Delta\sigma\,(eI_0F_{light})^{-1}$, where e, I_0, F_{Light}, and $\Delta\sigma$ are the unit charge of a single electron, incident photon density of excitation laser (photons m^{-2}), a correction (or filling) factor (m^{-1}), a transient photoconductivity, respectively. The change of conductivity is equivalent with $\Delta P_r/(AP_r)$, where ΔP_r, P_r, and A area change of reflected microwave power, a power of reflected microwave, and a sensitivity factor [S^{-1} m], respectively. Transient absorption spectroscopy (TAS) was performed by using THG of the same nanosecond laser as an excitation and a white light continuum from a Xe lamp as a probe light. The probe light was guided into a wide-dynamic-range streak camera (Hamamatsu C7700) which collects two-dimensional image of the spectrum and time profiles of light intensity.

Poly[styrene-ran-perylene-3,4,9,10-tetracarboxylic-mono(10-nonyldecyl)imide-mono(6-hexylacrylate) imide] (St-PDI copolymer) (**5**). Prior to the polymerization, styrene monomer was purified by distillation under reduced pressure. Distilled styrene monomer (5.0 g, 48.1mmol) and PDI **4** (0.025 g, 0.03 mmol or 0.05 g, 0.06 mmol) and anhydride toluene (6.0 mL) were placed in a flask and subjected to freeze-pump-throw at 3 times. Then azobisisobutyronitrile (AIBN) (6.6 mg, 0.04mmol) was added and stirred at 85 ˚C for 12h. The mixture was cooled, and then precipitated in acetone by 3 times. The pink precipitate was filtered and dried to give the random

copolymer **5** (yield: ca. 40 %). Elemental analysis found: C, 91.27; H, 7.57; N, 0.10 % and calc.: C, 91.00; H, 7.72; N, 0.29 %. From the calculations based on the copolymer structure, the weight percentages of incorporated PDI contents were determined to be 3 % and 10 %, respectively (thus, abbreviated as St-$PDI_{3\%}$ and St-$PDI_{10\%}$). The number-averaged molecular weight (M_n) and M_w of St-$PDI_{3\%}$ were 62 and 102 kg mol^{-1}, respectively, with a polydispersity index of 1.6. Those of St-$PDI_{10\%}$ were found to be 50 and 72 kg mol^{-1} with a polydispersity index of 1.4.

Poly[(methylmethacrylate)-ran-perylene-3,4,9,10-tetracarboxylic-mono(10-nonyldecyl)imide-mono(6-hexylacrylate) imide] (MMA-$PDI_{3\%}$ copolymer) (**6**). Prior to the polymerization, methyl methacrylate monomer was purified by distillation under reduced pressure. Distilled methyl methacrylate monomer (5.0 g, 48.1 mmol) and PDI **4** (0.025 g, 0.03 mmol) and anhydride toluene (8.5 mL) were placed in a flask and subjected to freeze-pump-throw at 3 times. Then azobisisobutyronitrile (AIBN) (7.0 mg, 0.04mmol) was added and stirred at 82 ˚C for 24h. The mixture was cooled, and then precipitated in acetone by 3 times. The pink precipitate was filtered and dried to give the random copolymer **6** (yield: ca. 50 %). Elemental analysis found: C, 67.10; H, 7.90; N, 0.10 % and calc.: C, 59.31; H, 7.47; N, 0.08 %. From the calculations based on the copolymer structure, the weight percentage of incorporated PDI contents was determined to be 3% (thus, abbreviated as MMA-$PDI_{3\%}$). M_n = 58 kg mol^{-1}, M_w = 98 kg mol^{-1} with a polydispersity index of 1.7.

Results and Discussion

Binary Blends of PS+P3HT and PMMA+P3HT

Electronic absorption spectra of binary polymer alloy of P3HT and PS (or PMMA) are shown in Fig. 1. All blend films display the primary broad peak at ca. 520 nm with two peaks at ca. 560 and 610 nm. These peaks are attributed to $S_0 \rightarrow S_1$ transitions with vibrating replicas of 0-2, 0-1, and 0-0, respectively, where the lowest energy peak (0-0) evolves as a result of planarization and/or intermolecular π-stack of P3HT.[49-51] Spano has modeled and calculated the effect of excitonic coupling and assigned the low and high energy bands to the aggregated and disordered P3HT chains, respectively.[52] In both P3HT+PS and P3HT+PMMA matrices in Fig. 1, the relative intensity of 610 nm peak was increased with P3HT concentration from 0.1 to 1 wt%. Upon further addition of P3HT, the intensity turned to decrease, resulting in the lowest intensity for the pristine P3HT. These results indicate that the planarity of P3HT backbone is higher for the polymer alloy than pristine film. Hellmann *et al.* reported the evolution of 0-0 peak in P3HT: poly(ethylene oxide) (PEO) blend and envisaged that polar matrices such as PEO planarize the backbone of a range of conjugated polymers.[53] They also found that the increase in 0-0 transition intensity entails the red shift with the increase of molecular weight of P3HT. In our studies, polar PMMA reveals the stronger and more red-shifted 0-0 peak than PS, in good agreement with the report of Hellmann *et al.* [53] Accordingly, PMMA is suggested to act as 'poorer solvent' than PS and facilitate the extension of π-conjugation length through the polymer-polymer interaction in the film formation process.

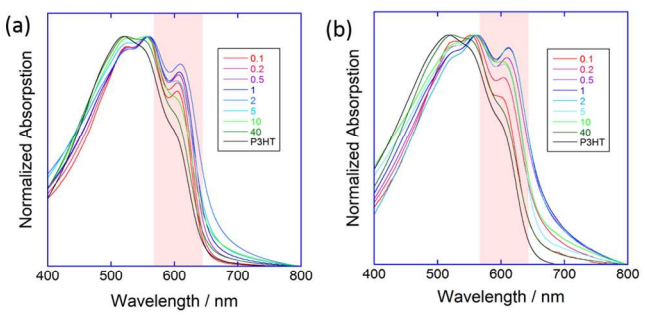

Fig. 1. Normalized electronic absorption spectra of P3HT dispersed in (a) PS and (b) PMMA matrices. Matrices : P3HT = 100 : 0.05-40.

FP-TRMC evaluations of the binary blend films of matrix+P3HT (100 : x in wt%, x = 0.05–40) were performed. The photoconductivity transient maxima ($\phi\Sigma\mu_{max}$, a product of quantum efficiency of charge carrier generation, ϕ, and sum of mobilities of positive and negative charge carriers, $\Sigma\mu = \mu_+ + \mu_-$) are plotted as a function of P3HT concentration in Fig. 2. Regardless of the insulating matrices (PS or PMMA), $\phi\Sigma\mu_{max}$ was increased almost linearly from P3HT = 0.1 to 10 wt% and saturated at the high concentrations. It should be noted that the absorption at the excitation wavelength (355 nm) is compensated in $\phi\Sigma\mu_{max}$, hence the change of $\phi\Sigma\mu_{max}$ is due to the variation in ϕ and/or $\Sigma\mu$. The increasing trend is similar to the previous FP-TRMC study of P3HT+PS processed from concentrated solutions.[54] On the other hand, the blend films of rather amorphous conjugated polymer and PS showed a flat dependence on the blend ratio.[55]

Fig. 3 shows surface morphologies of PS+P3HT and PMMA+P3HT films observed by AFM. At PS : P3HT = 100:0.1 (Fig. 3a), no clear phase separation is observed and the surface roughness is small as dictated from the small height scale bar. Therefore P3HT is assumed dispersed in PS matrix at 0.1 wt%. However, dot pattern appeared even at 0.2 wt% P3HT (Fig. 3b) and the diameter was increased with the P3HT concentration (0.2 ~ 5 wt% for Figs. 3c-3e). At 10 wt%, some of the dots are merged to form dumbbell-like structures (Fig. 3f). Apparently, the dots are mainly composed of P3HT and consistent with the phase-separated AFM images of PS:P3HT=100:100 film composed of P3HT island and PS sea.[45] In the case of PMMA+P3HT blends, the similar dot patterns and evolution of their sizes were observed over the whole range of P3HT concentration (Figs. 3g-3l). Although $\phi\Sigma\mu_{max}$ of PS and PMMA matrices are similar over the range from 0.1 to 10 wt% P3HT, the phase separation and electronic absorption spectra are somehow different among them, where PMMA promotes the aggregation and planarization of P3HT more significantly than PS.

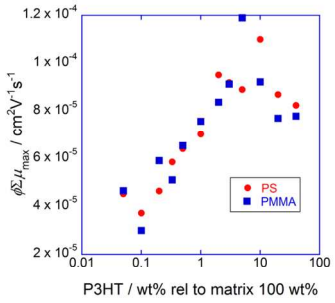

Fig. 2. $\phi\Sigma\mu_{max}$ of binary blend films of P3HT+PS (red circles) and P3HT+PMMA (blue squares) measured by FP-TRMC (λ_{ex} = 355 nm).

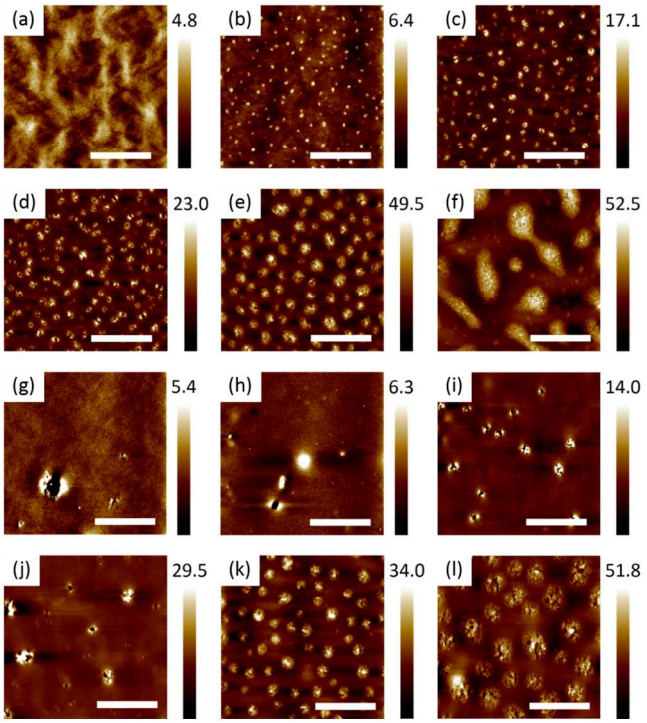

Fig. 3. AFM images of (a) - (f) PS+P3HT and (g) - (l) PMMA+P3HT blend films. The ratios of P3HT relative to 100 wt% matrix are (a) (g) 0.1, (b) (h) 0.2, (c) (i) 0.5, (d) (j) 1, (e) (k) 5, and (f) (l) 10. The colorized height scale bars are normalized at the respective images (the minimum is 0 nm). The white length scale bar is 5 μm.

Ternary Blends of PS+P3HT+PDI and PMMA+P3HT+PDI

To experimentally evaluate ϕ of P3HT+PS (or PMMA), we added swallow-tailed perylenediimide (PDI, **1** in Scheme 1) into the polymer alloy as the ternary component. This is because PDI is a representative electron acceptor,[56-58] and its radical anion has a characteristic absorption at 700–800 nm with the high extinction coefficient (> 10^4 dm^3 mol^{-1} cm^{-1}),[59,60] which is compatible with a direct detection using TAS. In addition, electron transfer from PDI to p-type polymer leads to the increase in ϕ, thus gaining strength in TRMC signal with higher signal-to-noise ratio. We have successfully utilized this scheme in the binary blends[61-63] and self-assemblies of PDI derivatives[64,65] to determine ϕ and $\Sigma\mu$.

Fig. 4a shows the plot of $\phi\Sigma\mu_{max}$ of FP-TRMC transients as a function of PDI concentration observed in ternary blend films of PS+P3HT+PDI (100:1:0.1–5 in wt%) (Kinetics are provided in Fig. S1). $\phi\Sigma\mu_{max}$ is increased with the PDI concentration up to 5 wt% by virtue to the enhanced charge separation efficiency via donor-acceptor framework, and then abruptly decreased at the high concentration. Such a decrease in the high PDI concentration region has been observed in P3HT+PDI (100 : >40 wt%),[61,62] in which the deterioration of P3HT lamellar by excessive PDI was identified as the main cause of decreased $\Sigma\mu$.

Fig. 4b shows the $\Sigma\mu$ in PS (or PMMA)+P3HT+PDI evaluated by combination of FP-TRMC and TAS under the low PDI concentration (0.5–5wt%). The TAS measurements of PMMA+P3HT+PDI at PDI > 5 wt% were not successful, because the film transparency was significantly degraded. The $\Sigma\mu$ in PMMA+P3HT with 1–3 wt% PDI were compelled to be almost constant at 0.3–0.35 cm^2 $V^{-1}s^{-1}$, while those of PS+P3HT are likely increasing from 0.13 cm^2 $V^{-1}s^{-1}$ at 0.5 wt% PDI to 0.25 cm^2 $V^{-1}s^{-1}$ at 5 wt% PDI. Self-assembled PDIs have been known as good electron transporting materials, where the highest values are on the order of 0.1–1 $cm^2V^{-1}s^{-1}$.[65-70] Therefore, the contribution of electron mobility of PDI might be responsible for the increase of $\Sigma\mu$ (= $\mu_+ + \mu_-$) observed in PS+P3HT+PDI.

Fluorescence spectra of binary blends of PS (or PMMA)+PDI

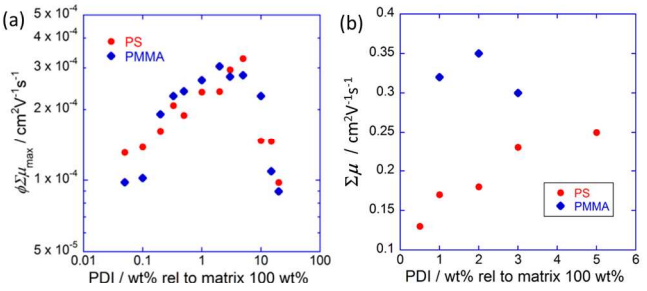

Fig. 4. TRMC results of simple ternary blends of PS (PMMA) : P3HT : PDI = 100 : 1 : 0.05–20. (a) Plot of $\phi\Sigma\mu_{max}$ vs PDI concentration. (b) Mobility ($\Sigma\mu$) determined by TRMC and TAS.

are shown in Figs. 5a and 5b, respectively. At the PDI concentration less than 0.5 wt%, the fluorescence spectra of blend films display two peaks at 530 and 570 nm, which are identical to those in $CHCl_3$ solution of isolated PDI molecule. However, further increase of PDI resulted in the appearance of the new broad peak at 600 nm. This peak is readily attributed to the excimer emission from PDI dimer.[71-73] Therefore PDIs are aggregated in insulating matrices even at the low PDI concentration of > 0.5 wt%. The situation was same in the ternary blends of PS (PMMA)+P3HT+PDI (Fig. S2).

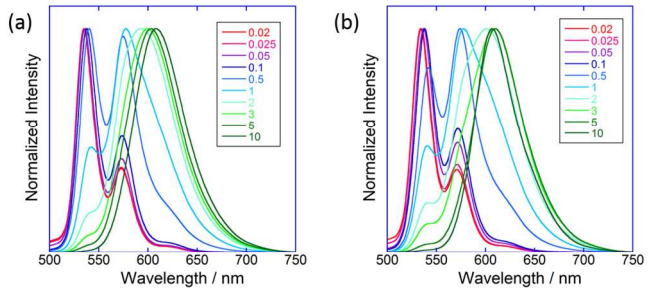

Fig. 5. Normalized fluorescence spectra (λ_{ex} = 355 nm) observed in PDI + (a) PS and (b) PMMA matrices. Matrices : PDI = 100 : 0.02–10.

Binary Blends of St-PDI+P3HT and MMA-PDI+P3HT

In order to remove the contribution of electron mobility of PDI aggregates, PDIs must be dispersed in polymer alloy. This drove us to design a random copolymer of PDI and insulator which can manipulate the electronic property of conjugated polymer and allow the evaluation of hole mobility without contribution of PDI electron mobility. To this end, St-PDI copolymers containing 3 and 10 wt%

PDI (St-PDI$_{3\%}$ and St-PDI$_{10\%}$) and MMA-PDI copolymer containing 3 wt% PDI (MMA-PDI$_{3\%}$) were synthesized according to the procedure in Scheme 1. The PDI ratio was determined by elemental analysis (see Experimental). Notably, the photoabsorption and fluorescence spectra of St-PDI$_{3\%}$ and MMA-PDI$_{3\%}$ films are similar to those of a dilute PDI solution, highlighting the dispersion of PDI molecules in the copolymer films (Figs. 6a-6f). This is sharp contrast to the distinct PDI excimer emission in the simple binary blend of PS (PMMA) and PDI at the same ratio (100:3). On the contrary, St-PDI$_{10\%}$ film showed the identical spectra to the blend of PS+PDI (100:10), indicative of the presence of PDI aggregates (Figs. 6c and 6d). Therefore, St-PDI$_{3\%}$ and MMA-PDI$_{3\%}$ can be used as the functional matrix to evaluate hole mobility by TRMC and TAS.

Fig. 7a shows the FP-TRMC transients of St-PDI$_{3\%}$+P3HT and PS+P3HT+3 wt% PDI. These transients are higher in intensity and longer in the lifetime than the binary blend of PS+P3HT (100:1) without PDI. This clearly indicates the electron transfer from P3HT to PDI covalently-bonded to the insulator and retarded charge recombination. However, the PS+P3HT+3 wt% PDI film shows a higher FP-TRMC signal than St-PDI$_{3\%}$+P3HT, although the component ratios are the same (PS:P3HT:PDI = 100:1:3). This is probably due to the unfavorable condensation of PDI near or inside the P3HT domain, facilitating the charge separation. $\phi\Sigma\mu_{max}$ of both alloys are increased with P3HT concentration by 4 ~ 5 times and

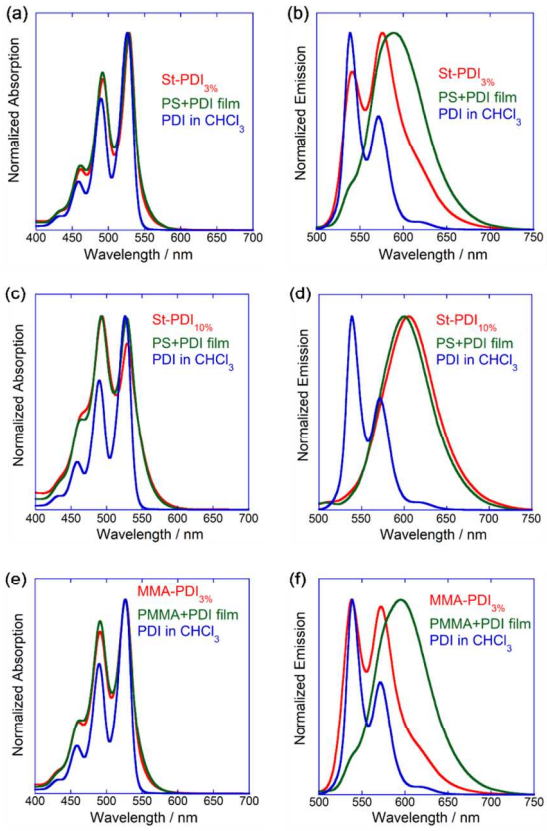

Fig. 6. Normalized photoabsorption (left panel) and fluorescence (right panel, λ_{ex} = 355 nm) spectra of (a)(b) St-PDI$_{3\%}$, (c)(d) St-PDI$_{10\%}$ and (e)(f) MMA-PDI$_{3\%}$ copolymers films (red lines). Photoabsorption and fluorescence spectra of simply-mixed films of PS+PDI (3% or 10%) and PMMA+PDI (3%) are drawn by the green lines. Those in $CHCl_3$ solution of 50 μmol dm^{-3} PDI are superimposed as the blue lines.

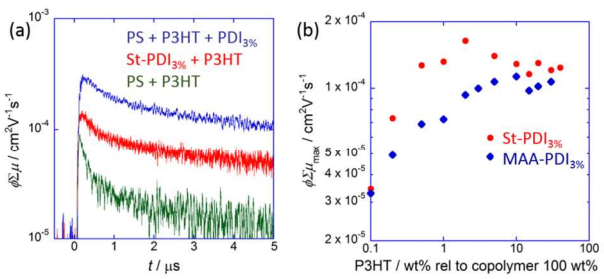

Fig. 7. (a) Conductivity transient observed in P3HT dispersed in PS-PDI$_{3\%}$, PS and PS + PDI matrix. The ratio was PS : P3HT = 100 : 1. (b) Dependence of maximum transient conductivity for P3HT concentration in St-PDI$_{3\%}$ and MMA-PDI$_{3\%}$ and. Matrices : P3HT = 100 : 0.1–40.

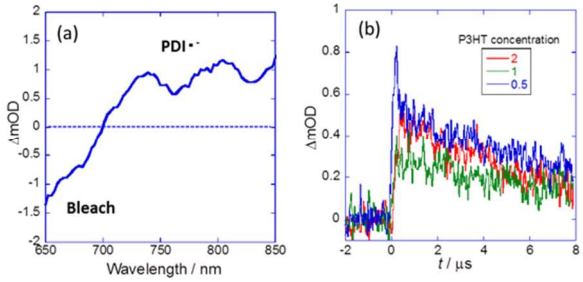

Fig. 8. TAS of P3HT+St-PDI$_{3\%}$ binary blend (λ_{ex} = 355 nm). (a) Transient absorption spectrum of St-PDI$_{3\%}$:P3HT=100:1 film at the pulse end. (b) Kinetic traces at. 795 nm in St-PDI$_{3\%}$:P3HT=100:0.5, 1, and 2 films. The spike at the pulse end seen in St-PDI$_{3\%}$:P3HT=100:0.5 is a fluorescence noise.

saturated at the relatively low P3HT concentrations of 0.5–2 wt% (Fig. 7b). Interestingly, the slope is steeper for St-PDI$_{3\%}$ than MMA-PDI$_{3\%}$. This could be rationalized by the size of P3HT domains as visualized in the AFM images of binary blend (Fig. 3), where the smaller size and large surface area of P3HT in PS are more advantageous than those of PMMA for charge separation at the P3HT/PDI interface.

Fig. 8a shows the transient absorption spectrum of St-PDI$_{3\%}$: P3HT = 100 : 1 film, in which the positive signal from ca. 700 to 800 nm is attributed to the PDI radical anion, in good agreement with the previous reports.[59-65] On the basis of kinetic traces of PDI radical anion at 795 nm (Fig. 8b), of which extinction coefficient is 4.96×10^4 mol^{-1} dm^3 cm^{-1},[59,60] the quantum efficiencies of the PDI radical anion generation (ϕ_{PDI}) were evaluated to be 2.5, 1.3, and 2.3 $\times 10^{-3}$ for the blend films of St-PDI$_{3\%}$: P3HT = 100 : 0.5, 1, and 2 wt%, respectively.

Accordingly, hole mobilities of P3HT were calculated to be 0.05 ± 0.01, 0.10 ± 0.02, and 0.07 ± 0.01 cm^2 V^{-1}s^{-1}, respectively. The average value is 0.07 ± 0.02 cm^2 V^{-1}s^{-1}, almost equal to the highest FET hole mobility of P3HT (0.1–0.2 cm^{2}V^{-1}s^{-1}),[74,75] while the typical FET mobilities of P3HT are usually lying on the orders of 10^{-3}–10^{-4} cm^{2}V^{-1}s^{-1}.[26-29] However, this TRMC mobility is one order higher than those found in benzene solution of P3HT measured by pulse-radiolysis TRMC (0.014 ~ 0.02 cm^{2}V^{-1}s^{-1} as the one dimensional mobility, their one thirds can be compared to those of the present results).[76,77] Solution is the most effective way to isolate conjugated polymer; however, the conformation of dissolved polymer chain might undergo distortion, leading to the decrease in

the intrachain mobility.[78] On the contrary, charge carrier mobilities of pristine P3HT films[61,62] and P3HT:fullerene blend film[79] are higher by a few factors (0.1–0.2 $cm^2V^{-1}s^{-1}$), suggesting that the film processing condition and counter material in the blend are critical to the local mobility relating to the conformation and intermolecular interaction of the semiconductors. TAS signal of PDI radical anion was unable to be observed in MMA-$PDI_{3\%}$ and P3HT blend, because the ϕ_{PDI} in the MMA-$PDI_{3\%}$ matrix was smaller than the noise level of our TAS system. Therefore, hole mobility of P3HT in MMA-$PDI_{3\%}$ matrix is presumed higher than that in St-$PDI_{3\%}$ at least by a few factors. PS and PMMA are often of choices as a gate insulating materials in OFET devices, and considerable suppression of charge carrier mobility has been reported via the localization of charge carriers by dipolar effects at the insulator–semiconductor interfaces.[80-82] Clear localization of carriers in the long-range translational motion was observed and measured by FET fabrication of binary mixture of semiconducting polymers with dipoles[35,83], thus the effects of the dipoles of PS and PMMA are of interest in the present mixture systems. Here, the mobility of charge carriers are estimated as a result of non-translational local motion induced by the alternating electric field of microwave probes, and the effects of the local dipoles of the surrounding media can be estimated in terms of the complex dielectric constants induced by an injection of charge carriers, hence by tracing transient dielectric dispersion. The frequency of microwave probes is set at ~ 10 GHz, where the dielectric dispersion of the present mixture systems can be represented by Debye-type one as follows,

$$\varepsilon(\omega) = \varepsilon_\infty + (\varepsilon_S - \varepsilon_\infty)/(1 + i\omega\tau) \quad (1).$$

Here, ε_S, ε_∞, and τ are the static dielectric constant of the media, the constant at the high frequency limit, and relaxation time, respectively. PMMA was used as the dipolar matrices in the glassy state at room temperature, in which multi-mode dipolar relaxation had been observed with considerable distribution of τ. Taking the distribution into accounts with the scaling parameters of α and β, the following Negami-type expression of a form provides a better interpretation to the dielectric dispersion of the media,

$$\varepsilon(\omega) = \varepsilon_\infty + (\varepsilon_S - \varepsilon_\infty)/\{1 + (i\omega\tau)^\beta\}^\alpha \quad (2).$$

In a PS matrix, the relative dielectric constants was reported as 2.5 with small dependence on ω. In contrast, PMMA exhibited the higher value of the constant with several characteristic τ corresponding the local modes such as β' and/or β'' relaxation of the pendant ester groups. However the values of τ have been reported as 10^{-6} s, leading to a convergent dielectric constant as ~ 2.7 at around 9 GHz from eq. (2). This is the case giving the small effects of the dipoles in TRMC measurement, securing quantitative analysis of the local charge carrier mobility in the present system. Indeed, the high $\Sigma\mu$ of 0.3–0.35 $cm^2\ V^{-1}s^{-1}$ is observed in the simple blend of PMMA+P3HT+PDI (Fig. 4b), iterating that the large driving force of phase separation between nonpolar P3HT and polar PMMA leads to the planarization and strong intermolecular stacking in the P3HT domains.

The $\Sigma\mu$ of 0.07 ± 0.02 $cm^2V^{-1}s^{-1}$ evaluated in St-$PDI_{3\%}$: P3HT = 100 : 0.5–2 is lower than that in the ternary blend of PS+P3HT+2 wt% PDI (ca. 0.17 $cm^2\ V^{-1}s^{-1}$), where the latter was expected to include the electron mobility of PDI aggregates. It is noteworthy that the difference of these $\Sigma\mu$ is 0.1 (= 0.17 - 0.07) $cm^2V^{-1}s^{-1}$, which is coincident with the typical TRMC mobility of π-stacked PDIs (0.1–0.2 $cm^2V^{-1}s^{-1}$).[65,66] This supports our claim on the role of PDI-appended insulator to remove contribution of electron mobility from the TRMC evaluation. Thus, we developed a new scheme to evaluate local hole mobility of conjugated polymer in insulating electron-accepting matrix specially-designed for FP-TRMC. This matrix could be applicable to a wide range of p-type polymers and of help to investigate their potential charge transport properties.

Conclusion

Polymer alloy comprising P3HT and insulator (PS or PMMA) were investigated by AFM, FP-TRMC, and TAS. We found that the planarity of P3HT was enhanced more in polar PMMA than in nonpolar PS. Accordingly, the local mobilities ($\Sigma\mu$) of the former was higher (0.3–0.35 $cm^2V^{-1}s^{-1}$) than the latter (0.13–0.25 $cm^2V^{-1}s^{-1}$). This highlights the unique role of insulating matrix to modulate the backbone configuration of crystalline polymer. However, these mobilities were assumed to include electron mobilities of PDI aggregates which were blended into the polymer alloy to evaluate ϕ using TAS. We therefore designed the random copolymers of St-$PDI_{3\%}$ and MMA-$PDI_{3\%}$. The PDIs were found mostly dispersed in the film states as evident from the absence of PDI excimer emission. The hole mobility in the St-$PDI_{3\%}$+P3HT blend was determined to be 0.07 ± 0.02 $cm^2V^{-1}s^{-1}$ on average, which is equivalent to the value calculated by extracting typical electron mobility of π-stacked PDI in the literatures (0.1–0.2 $cm^2V^{-1}s^{-1}$) from the $\Sigma\mu$ of PS+P3HT+PDI (0.13–0.25 $cm^2V^{-1}s^{-1}$). Because of the technical reason, hole mobility in the MMA-$PDI_{3\%}$+P3HT blends was not evaluated; however, the value is expected much higher than that in St-$PDI_{3\%}$. The combination of FP-TRMC/TAS and polymer alloy offers a facile and effective way towards not only fully-experimental evaluation of hole mobility but also manipulating the backbone conformation and aggregation structure of conjugated polymer.

Acknowledgements

This work was supported by the KAKENHI from the Ministry of Education, Culture, Sports, Science and Technology (MEXT), Japan (No. 23108710, 25288084, 26249145, and 26102011). T. F. acknowledges the financial support of The Japan Society for the Promotion of Science (JSPS) scholarship.

References

1 A. J. Heeger, *Adv. Mater.,* 2014, **26**, 10.
2 S. D. Dimitrov and J. R. Durrant, *Chem. Mater.,* 2014, **26**, 616.
3 C. Gao, L. Wang, X. Li and H. Wang, *Polym. Chem.,* 2014, **5**, 5200.
4 H. Zhang and B. Tieke, *Polym. Chem.,* 2014, **5**, 6391.
5 S. C. Price, A. C. Stuart, L. Yang, H. Zhou and W. You, *J. Am. Chem. Soc.*. 2011, **133**, 4625.
6 B. C. Thompson and J. M. J. Fréchet, *Angew. Chem. Int. Ed.,* 2008, **47**, 58.
7 C. J. Brabec, N. S. Sariciftci and J. C. Hummelen, *Adv. Funct. Mater.,* 2001, **11**, 15.
8 C. R. Newman, C. D. Frisbie, D. A. da Silva Filho, J.-L. Brédas, P. C. Ewbank and K. R. Mann, *Chem. Mater.,* 2004, **16**, 4436.
9 R. Mondal, N. Miyaki, H. A. Becerril, J. E. Norton, J. Parmer, A. C. Mayer, M. L. Tang, J.-L. Brédas, M. D. McGehee and Z. Bao, *Chem. Mater.,* 2009, **21**, 3618.
10 T. Umeda, D. Kumaki and S. Tokito, *J. Appl. Phys.,* 2009, **105**, 024516.

11 D. Boudinet, M. Benwadih, S. Altazin, J.-M. Verilhac, E. De Vito, C. Serbutoviez, G. Horowitz and A. Facchetti, *J. Am. Chem. Soc.,* 2011, **133**, 9968.
12 K. Takimiya, S. Shinamura, I. Osaka and E. Miyazaki, *Adv. Mater.,* 2011, **23**, 4347.
13 L. Biniek, B. C. Schroeder, C. B. Nielsen and I. McCulloch, *J. Mater. Chem.,* 2012, **22**, 14803.
14 Y. Koizumi, M. Ide, A. Saeki, C. Vijayakumar, B. Balan, M. Kawamoto and S. Seki, *Polym. Chem.,* 2013, **4**, 484.
15 J. H. Burroughes, D. D. C. Bradley, A. R. Brown, R. N. Marks, K. Mackay, R. H. Friend, P. L. Burns and A. B. Holmes, *Nature,* 1990, **347**, 539.
16 R. H. Friend, R. W. Gymer, A. B. Holmes, J. H. Burroughes, R. N. Marks, C. Taliani, D. D. C. Bradley, D. A. Dos Santos, J. L. Brédas M. Logdlund and W. R. Salaneck, *Nature,* 1999, **397**, 121.
17 C. D. Dimitrakopoulos and P. R. T. Malenfant, *Adv. Mater.,* 2002, **14**, 99.
18 A. C. Arias, J. D. MacKenzie, I. McCulloch, J. Rivnay and A. Salleo, *Chem. Rev.,* 2010, **110**, 3.
19 L. Xiao, Z. Chen, B. Qu, J. Luo, S. Kong, Q. Gong and J. Kido, *Adv. Mater.,* 2011, **23**, 926.
20 L. Li, T.-Q. Hu, C.-R. Yin, L.-H. Xie, Y. Yang, C. Wang, J.-Y. Lin, M.-D. Yi, S.-H. Ye and W. Huang, *Polym. Chem.,* 2015, **6**, 983
21 F. Padinger, R. S. Rittberger and N. S. Sariciftci, *Adv. Funct. Mater.,* 2003, **13**, 85.
22 G. Li, V. Shrotriya, Y. Yao and Y. Yang, *J. Appl. Phys.,* 2005, **98**, 043704.
23 S. Berson, R. De Bettignies, S. Bailly and S. Guillerez, *Adv. Funct. Mater.,* 2007, **17**, 1377.
24 Y. He, H.-Y. Chen, J. Hou and Y. Li, *J. Am. Chem. Soc.,* 2010, **132**, 1377.
25 H. Yang, T. J. Shin, L. Yang, K. Cho, C. Y. Ryu and Z. Bao, *Adv. Funct. Mater.,* 2005, **15**, 671.
26 G. Wang, D. Moses, A. J. Heeger, H.-M. Zhang, M. Narasimhan and R. E. Demaray, *J. Appl. Phys.,* 2004, **95**, 316
27 M. Surin, Ph. Leclére, R. Lazzaroni, J. D. Yuen, G. Wang, D. Moses, A. J. Heeger, S. Cho and K. Lee, *J. Appl. Phys.,* 2006, **100**, 033712.
28 H. Sirringhaus, P. J. Brown, R. H. Friend, M. M. Nielsen, K. Bechgaard, B. M. W. Langeveld–Voss, A. J. H. Spiering, R. A. J. Janssen, E. W. Meijer, P. Herwig and D. M. De Leeuw, *Nature,* 1999, **401**, 685.
29 L. Qiu, J. A. Lim, X. Wang, W. H. Lee, M. Hwang and K. Cho, *Adv. Mater.,* 2008, **20**, 1141.
30 Y. Xu, J. Liu, H. Wang and Y. Han, *RSC Adv.,* 2013, **3**, 17195.
31 S.-C. Liufu, L.-D. Chen, Q. Yao and C.-F. Wang, *Appl. Phys. Lett.,* 2007, **90**, 112106.
32 H. Kang, M. A. Uddin, C. Lee, K.-H. Kim, T. L. Nguyen, W. Lee, Y. Li, C. Wang, H. Y. Woo and B. J. Kim, *J. Am. Chem. Soc.,* 2015, **137**, 2359.
33 D. Mori, H. Benten, I. Okada, H. Ohkita and S. Ito, *Energy Environ. Sci.,* 2014, **7**, 2939.
34 T. Earmme, Y.-J. Hwang, N. M. Murari, S. Subramaniyan and S. A. Jenekhe, *J. Am. Chem. Soc.,* 2013, **135**, 14960.
35 A. Babel and S. A. Jenekhe, *Macromolecules,* 2004, *37*, 9835.
36 S. Goffri, C. Müller, N. Stingelin-Stutzmann, D. W. Breiby, C. P. Radano, J. W. Andreasen, R. Thompson, R. A. J. Janssen, M. M. Nielsen, P. Smith and H. Sirringhaus, *Nature Mater*., 2006, **5**, 950.
37 L. Qiu, W. H. Lee, X. Wang, J. S. Kim, J. A. Lim, D. Kwak, S. Lee and K. Cho, *Adv. Mater*., 2009, **21**, 1349.
38 K. Sugiyasu, Y. Honsho, R. M. Harrison, A. Sato, T. Yasuda, S. Seki and M. Takeuchi, *J. Am. Chem. Soc.,* 2010, **132**, 14754.
39 J. Terao, Y. Tanaka, S. Tsuda, N. Kambe, M. Taniguchi, T. Kawai, A. Saeki and S. Seki, *J. Am. Chem. Soc.,* 2009, **131**, 18046.
40 J. M. Warman, J. Piris, W. Pisula, M. Kastler, D. Wasserfallen and K. Müllen, *J. Am. Chem. Soc.,* 2005, **127**, 14257.
41 F. C. Grozema and L. D. A. Siebbeles, *J. Phys. Chem. Lett.,* 2011, **2**, 2951.
42 A. Saeki, Y. Koizumi, T. Aida and S. Seki, *Acc. Chem. Res.,* 2012, **45**, 1193.
43 S. Seki, A. Saeki, T. Sakurai and D. Sakamaki, *Phys. Chem. Chem. Phys.,* 2014, **16**, 11093.
44 M. J. Bird, O. G. Reid, A. R. Cook, S. Asaoka, Y. Shibano, H. Imahori, G. Rumbles and J. R. Miller, *J. Phys. Chem. C,* 2014, **118**, 6100.
45 S. Honda, H. Ohkita, H. Benten and S. Ito, *Adv. Energy Mater.,* 2011, **1**, 588.
46 Q. Zhang, A. Cirpan, T. P. Russell and T. Emrick, *Macromolecules,* 2009, **42**, 1079.
47 L. D. Wescott and D. L. Mattern, *J. Org. Chem.,* 2003, **68**, 10058.
48 R. T. Pon, *Tetrahed. Lett.,* 1991, **32**, 1715.
49 G. Li, V. Shrotriya, J. Huang, Y. Yao, T. Moriarty, K. Emery and Y. Yang, *Nature Mater.,* 2005, **4**, 864.
50 J. Y. Kim, S. H. Kim, H.-H. Lee, K. Lee, W. Ma, X. Gong and A. J. Heeger, *Adv. Mater.,* 2006, **18**, 572.
51 Y. Kim, S. Cook, S. M. Tuladhar, S. A. Choulis, J. Nelson, J. R. Durrant, D. D. C. Bradley, M. Gile, I. McCulloch, C.-S. Ha and M. Ree, *Nature Mater.,* 2006, **5**, 197.
52 F. C. Spano, *J. Chem. Phys.,* 2005, **122**, 234701.
53 C. Hellmann, F. Paquin, N. D. Treat, A. Bruno, L. X. Reynolds, S. A. Haque, P. N. Stavrinou, C. Silva and N. Stingelin, *Adv. Mater.,* 2013, **25**, 4906.
54 T. Fukumatsu, A. Saeki and S. Seki, *J. Photopolym. Sci. Tech.,* 2012, **25**, 665.
55 A. Saeki, T. Fukumatsu and S. Seki, *Macromolecules,* 2011, **44**, 3416.
56 B. A. Jones, A. Facchetti, M. R. Wasielewski and T. J. Marks, *J. Am. Chem. Soc.,* 2007, ***129***, 15259.
57 N. Vân Anh, R. Schlosser, M. M. Groeneveld, I. H. M. van Stokkum, F. Würthner and R. M. Williams, *J. Phys. Chem. C,* 2009, **113**, 18358.
58 V. Kamm, G. Battagliarin, I. A. Howard, W. Pisula, A. Mavrinskiy, C. Li, K. Müllen and F. Laquai, *Adv. Energy Mater.,* 2011, **1**, 297.
59 W. E. Ford, H. Hiratsuka and P. V. Kamat, *J. Phys. Chem.,* 1989, **93**, 6692.
60 D. Gosztola, M. P. Niemczyk, W. Svec, A. S. Lukas and M. R. Wasielewski, *J. Phys. Chem. A,* 2000, **104**, 6545.
61 A. Saeki, S. Ohsaki, S. Seki and S. Tagawa, *J. Phys. Chem. C,* 2008, **112**, 16643.
62 Y. Yasutani, A. Saeki, T. Fukumatsu, Y. Koizumi and S. Seki, *Chem. Lett.,* 2013, **42**, 19.
63 S. Prasanthkumar, A. Saeki, S. Seki and A. Ajayaghosh, *J. Am. Chem. Soc.,* 2010, **132**, 8866.
64 W.-S. Li, A. Saeki, Y. Yamamoto, T. Fukushima, S. Seki, N. Ishii, K. Kato, M. Takata and T. Aida, *Chem. –Asian J.,* 2010, **5**, 1566.
65 S. Yagai, M. Usui, T. Seki, H. Murayama, Y. Kikkawa, S. Uemura, T. Karatsu, A. Kitamura, S. Asano and S. Seki, *J. Am. Chem. Soc.,* 2012, **134**, 7983.
66 C. W. Struijk, A. B. Sieval, J. E. J. Dakhorst, M. van Dijk, P. Kimkes, R. B. M. Koehorst, H. Donker, T. J. Schaafsma, S. J. Picken, A. M. van de Craats, J. M. Warman, H. Zuilhof and E. J. R. Sudhölter, *J. Am. Chem. Soc.,* 2000, **122**, 11057.
67 Y. Wen and Y. Liu, *Adv. Mater.,* 2010, **22**, 1331.
68 J. Soeda, T. Uemura, Y. Mizuno, A. Nakao, Y. Nakazawa, A. Facchetti and J. Takeya, *Adv. Mater.,* 2011, **23**, 3681.
69 A. Lv, S. R. Puniredd, J. Zhang, Z. Li, H. Zhu, W. Jiang, H. Dong, Y. He, L. Jiang, Y. Li, W. Pisula, W. Meng, W. Hu and Z. Wang, *Adv. Mater.,* 2012, **24**, 2626.
70 M. Funahashi and A. Sonoda, *Org. Electronics,* 2012, **13**, 1633.
71 W. E. Ford and P. J. Kamat, *J. Phys. Chem.,* 1987, **91**, 6373.
72 Z. Chen, V. Stepanenko, V. Dehm, P. Prins, L. D. A. Siebbeles, J. Seibt, P. Marquetand, V. Engel and F. Würthner, *Chem. Eur. J.,* 2007, **13**, 436.
73 T. E. Kaiser, V. Stepanenko and F. Würthner, *J. Am. Chem. Soc.,* 2009, ***131***, 6719.

74 H. Sirringhaus, N. Tessler and R. H. Friend, *Science,* 1998, *280*, 1741.
75 G. Wang, J. Swensen, D. Moses and A. J. Heeger, *J. Appl. Phys.,* 2003, **93**, 6137.
76 F. C. Grozema, L. D. A. Siebbeles, J. M. Warman, S. Seki, S. Tagawa and U. Scherf, *Adv. Mater.,* 2002, **14**, 228.
77 F. C. Grozema and J. M. Warman, *Radiat. Phys. Chem.,* 2005, *74*, 234.
78 S. Asaoka, N. Takeda, T. Iyoda, A. R. Cook and J. R. Miller, *J. Am. Chem. Soc.,* 2008, **130**, 11912.
79 A. Saeki, M. Tsuji, S. Seki, *Adv. Energy Mater.,* 2011, **1**, 661.
80 Y. Honsho, T. Miyakai, T. Sakurai, A. Saeki and S. Seki, *Sci. Rep.* **2013**, *3*, 3182.
81 W. Choi, T. Miyakai, T. Sakurai, A. Saeki, M. Yokoyama and S. Seki, *Appl. Phys. Lett.* **2014**, *105*, 033302.
82 Y. Tsutsui, T. Sakurai, S. Minami, K. Hirano, T. Satoh, W. Matsuda, K. Kato, M. Takata, M. Miura and S. Seki, *Phys. Chem. Chem. Phys.* **2015**, *17*, 9624.
83 G. Lu, J. Blakesley, S. Himmelberger, P. Pingel, J. Frisch, I. Lieberwirth, I. Salzmann, M. Oehzelt, R. Di Pietro, A. Salleo, N. Koch and D. Neher, *Nat. Commun.*, 2013, **4**, 1588

TOC graphic